

See discussions, stats, and author profiles for this publication at: <https://www.researchgate.net/publication/372854792>

A Quantum Machine Learning Approach for Detecting User Locations

Article · August 2023

CITATIONS

0

READS

2

5 authors, including:



Erkan Guler

Giresun University

13 PUBLICATIONS 49 CITATIONS

SEE PROFILE



Muhammet Talha Kakiz

Osmaniye Korkut Ata university

9 PUBLICATIONS 36 CITATIONS

SEE PROFILE

A Quantum Machine Learning Approach for Detecting User Locations

Received: 30 February 2023; Accepted: 5 March 2023

Research Article

Erkan Güler

Department of Computer Engineering
Giresun University
Giresun, Türkiye
erkan.guler@giresun.edu.tr
ORCID: 0000-0001-7225-0859

Muhammet Talha Kakız

Department of Computer Engineering
Osmaniye Korkut Ata University
Osmaniye, Türkiye
mtalhakakiz@osmaniye.edu.tr
ORCID: 0000-0003-4928-6559

Tuğrul Çavdar

Department of Computer Engineering
Karadeniz Technical University
Trabzon, Türkiye
ulduz@ktu.edu.tr
ORCID: 0000-0003-3656-9592

Faruk Baturalp Günay

Department of Computer Engineering
Atatürk University
Erzurum, Türkiye
baturalp@atauni.edu.tr
ORCID: 0000-0001-5472-3608

Burcu Şanal

Vocational School of Technical
Sciences
Recep Tayyip Erdoğan University
Rize, Türkiye
burcu.sanal@erdogan.edu.tr
ORCID: 0000-0002-4541-7622

Abstract—Quantum Machine Learning methods are becoming a key component for various types of tasks making predictions or decisions based on datasets. Recent efforts and researches on quantum computing point out the significance of quantum speedup advantage, especially for learning processes that require enormous amount of computational resources. Advances in both quantum hardware design and hybrid quantum-classical software frameworks accommodate a paradigm shift from classical to quantum. In consideration with this quantum leap notion, we investigate the capability of variational quantum algorithms (VQA) on a real world problem of user localization dealing with the binary classification task. This paper introduces a VQA with four variants that differ in the number of layers related to the variational quantum circuit (VQC) part of the VQA. The samples from a publicly available user localization dataset are first preprocessed through padding, scaling and normalization. Next, they are mapped into three qubit quantum states using amplitude encoding as a data embedding scheme. Unitary transformation of the mapped quantum data in the VQC is followed by a measurement in computational basis to produce predictions for the labels. The error between true and predicted labels is computed in a classical manner and a cost function minimization process is executed with the aid of gradient descent algorithm. The updated training parameters from the optimization stage are fed into the VQC and this process is repeated until the learnable parameters converge. The simulation results demonstrate that the designed VQA for binary classification achieves an accuracy value of 99% in the training phase. Moreover, the ratio of predicted labels to true labels approaches to 93% during the validation of actual user locations based on the signal strength received from the routers that are positioned at different places in a facility.

Keywords—quantum machine learning, user localization, variational quantum algorithm, variational quantum circuit, amplitude encoding

I. INTRODUCTION

Quantum computing is a fascinating computer science field that has attracted the attention of scientists and professionals from various disciplines. Although the intense curiosity might be reasoned in a variety of ways, the foremost argument that can be raised against the profound interest in

this emerging technology is twofold: (1) Current methods in producing classical computers are in the eve of encountering size related problems. As electronic devices get smaller, quantum effects start to influence the precise functioning of computers [1]. (2) Quantum computation is proved to be much more efficient than its classical counterpart for some computational tasks of practical importance such as integer factorization [2], search for an element in unstructured database [3] and simulation of quantum systems [4].

The massive computational power of quantum computers has led major IT companies (e.g., IBM, Google, and D-Wave) to produce quantum hardware, some of which are exposed via cloud platforms. However, currently available quantum computers are in infancy period suffering from environmental noise and it is the major difficulty in building large-scale quantum computers [5]. Noise causes disturbances in the state of the basic information unit *quantum bit* (qubit) and affects the computational accuracy. Due to the issue of noise, the current state of the art in the fabrication of quantum processors is described as Noisy Intermediate Scale Quantum (NISQ) era [6], where intermediate scale refers to the qubit number used in quantum computers varying from 50 to a few hundred qubits. With the introduction of NISQ devices, researchers have started to investigate the potential uses of quantum computers in various fields including finance, robotics, cybersecurity, energy management and chemical engineering [7]. Among all the research areas in relation to the quantum computing, the quantum machine learning (QML) is one of the most promising one [8] and has become an active subfield of quantum computing research [9].

The main goal of Machine Learning (ML), which spans a wide range of disciplines and has numerous applications, is to learn from data. Statistical patterns in data are recognized and inferences are drawn during the learning process. Despite advances in GPUs for parallel processing, the volume of data generated recently exceeds the computational power of conventional computers [10]. Thus, quantum computing has opened up a new playground for machine learning namely QML, which investigates the approaches and methods that harness the fields of machine learning and quantum computing [11]. Researchers are focused on using the power

of quantum computers to solve machine learning problems at considerably faster rates than classical counterparts [12] with the aid of QML.

Variational quantum algorithms (VQA), also referred to as hybrid quantum-classical algorithms, are described as encouraging approaches that employ NISQ devices to perform QML and to address real world problems that are beyond the capabilities of classical computers [13]. Variational Quantum Eigensolver and Quantum Approximate Optimization Algorithm are examples of the VQA algorithms. In this framework, computational tasks are split between quantum and classical resources. The quantum part of the framework employs parameterized (variational) quantum circuits to predict the labels of the training data through approximations. On the other hand, the classical part iteratively executes the update routines for the parameters of the parametrized quantum circuit (PQC) [14]. The functionality of these parameters bears resemblance to the weights of an artificial neural network. The fault-tolerant quantum computers are still an open research issue. However, the effect of noise on NISQ devices can be mitigated by keeping the circuit depth shallow [15]. This strategy provides an advantage for the QML methods using PQCs.

ML methods are broadly grouped under three different types: Supervised learning, unsupervised learning and reinforcement learning. In this work, we address one of the ML methods, which is binary classification as a supervised learning approach. We aim at supplying the practical implementation of required QML-based classification method by tackling a problem known as user localization in an indoor environment. Also, we investigate the layered structure of the utilized VQC in the context of improved classification outcomes.

This paper is organized as follows: We give a brief literature overview in Section II. The background about the concepts of quantum computation and quantum circuits is covered in Section III, while Section IV deals with the proposed quantum circuit for the classification problem. The results and the corresponding interpretations are drawn in Section V. We conclude the paper with summary and future research directions in Section VI.

II. RELATED WORK

The authors of [16] propose a model for the indoor localization of users in a building. The Received Signal Strength Indicator (RSSI) data gathered from the user equipments is exploited to perform an estimation on indoor occupancy count. The occupancy issue is handled as a binary classification problem, for which the following machine learning algorithms are used: k-nearest neighbor, decision tree, support vector machine and logistic regression. Recurrent neural networks are also studied in regard to locating people or objects within a building. The research presented in [17] focuses on a learning algorithm named as Speed Conscious Recurrent Neural Network, which provides a way to predict the locations. Furthermore, the authors propose fault-tolerant approaches such as nearest RSSI and most recent RSSI with the aim of improving the location accuracy.

In [18], remote health monitoring and smart homes are stated as some of the IoT applications, which are in need of location estimation techniques. The authors introduce a device-free localization system consisted of passive infrared

(PIR) sensors. The data collected through PIR sensors is evaluated with deep learning algorithms such as convolutional neural networks and recurrent neural networks in order to estimate the user locations. Variances in received signal strength from user terminals, device heterogeneity and environment complexity such as obstacles in a building can cause challenges on the localization problem. Due to this fact, the work in [19] introduces a high adaptability indoor localization method using a backpropagation neural network. The devised approach reveals the similarities on the received signal strength fingerprints and provides an improved localization accuracy.

One of the first researches related to classification problem using quantum computers is included in [20]. The authors exploit the idea of Hamming Distance measurement on a quantum computer in order to classify the handwritten digits from the well-known MNIST dataset.

As an effort of adapting the deep neural networks into the quantum realm, the work in [21] introduces a variational quantum deep neural network model for the problem of image classification. The proposed three classifiers are executed on both a simulation platform and a quantum hardware. The experimental results for the binary classification of the handwritten digits in the MNIST database achieved an accuracy of 100%, while ten-label classification task for the RGB images from the UCI database obtained an accuracy rate of 91%.

It is obvious that the earlier implementations of QML algorithms have mainly benefited from the MNIST images. The advances in the parametrized quantum circuits have led the researchers to investigate the potential of PQCs for other disciplines such as geoscience and medicine. In [22], the classification of satellite images is investigated. The experimental results show that the employed PQC performs better than a classic deep learning method. The effort of malaria disease diagnosis with the aid of quantum machine learning presented in [23] is one of the first instances delving into the detection of parasites that cause lethal illnesses. The work mainly focuses on the recognition of the malaria parasites by identifying the dots on the red blood cell images. The developed classification scheme emphasizes the significance of disease detection with fewer learnable parameters and features. The issue on the reduction of training parameters is also investigated by the authors of [24]. In comparison to the classical machine learning approaches, variational quantum circuit architecture is stated to pose an advantage in terms of parameter size.

As can be seen, majority of the classification approaches in the field of quantum machine learning is about image classification, which is also intensively discussed in classical supervised learning context. However, it is crucial to attempt broadening the implementation domain of parametrized quantum circuits by taking the real world samples other than images into consideration.

III. BACKGROUND

A. Quantum Bit (Qubit)

The information in classical computation is represented by bits, where one bit can be in one of the two states: 0 or 1. On the other hand, the basic unit of information in quantum computation is *qubit*. A qubit can be considered as a two-level system spanned by two orthogonal states. By definition, two

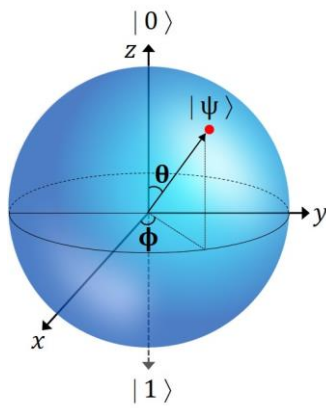


Fig. 1. Geometric representation of a qubit on Bloch Sphere

states are said to be orthogonal if their inner product is equal to the scalar value 0. In a 1-qubit system, those states satisfying the orthogonality condition form a basis known as *computational basis* and are denoted by:

$$|0\rangle = \begin{bmatrix} 1 \\ 0 \end{bmatrix}, |1\rangle = \begin{bmatrix} 0 \\ 1 \end{bmatrix} \quad (1)$$

The notation $|\cdot\rangle$ describing the state of a quantum system is a shorthand for writing the column vectors and referred to as *ket notation*. A generic qubit state $|\psi\rangle$ can be in a *superposition* of the computational basis states and is formulated as a linear combination of $|0\rangle$ and $|1\rangle$:

$$|\psi\rangle = \alpha|0\rangle + \beta|1\rangle = \begin{bmatrix} \alpha \\ \beta \end{bmatrix} \quad (2)$$

where α, β are complex numbers and the amplitudes of the state $|\psi\rangle$. Since each state vector is a unit vector in a complex vector space named as Hilbert space, the following condition must hold:

$$|\alpha|^2 + |\beta|^2 = 1 \quad (3)$$

Hence, each state $|\psi\rangle$ has to be normalized according to the given formula above. When a state is measured in the computational basis, it collapses into either $|0\rangle$ state with a probability of $|\alpha|^2$ or $|1\rangle$ state with a probability of $|\beta|^2$. The measurement in a quantum system changes the state implying that the original information is lost.

The utmost power of quantum computation is based on (2) due to the fact that each qubit is represented by two complex amplitudes, which are theoretically capable of taking infinitely many different values. As a consequence, a quantum system with n qubits is specified by 2^n amplitudes, providing a natural way of storing and manipulating enormous amount of information simultaneously, usually referred to as *quantum parallelism*. The generalization of a 1-qubit state $|\psi\rangle$ to n -qubits is as follows:

$$|\psi\rangle = \sum_{i=0}^{2^n-1} \alpha_i |i\rangle \quad (4)$$

where the normalization conditions is satisfied:

$$\sum_{i=0}^{2^n-1} |\alpha_i|^2 = 1, \quad \alpha_i \in \mathbb{C} \quad (5)$$

A qubit can be geometrically visualized on the surface of a 3-dimensional unit sphere called as Bloch Sphere (Fig. 1).

The state $|\psi\rangle$ is associated with two spherical coordinates and its ket notation from (2) can be rewritten in terms of θ and ϕ :

$$|\psi\rangle = \cos\left(\frac{\theta}{2}\right)|0\rangle + e^{i\phi} \sin\left(\frac{\theta}{2}\right)|1\rangle \quad (6)$$

B. Quantum Gates

Classical bits are altered with logical gates. The number of bits that are manipulated depends on the type of deployed gate. For instance, NOT gate operates on only one bit flipping the input bit, whereas two bits are fed into the AND gate and the result is only one bit. Note that the classical logical gates are not reversible at all. It is obvious that it is not possible to deduce the input bits of an AND gate from the output bit.

Just like the logical gates, the transformation of qubits are realized through quantum gates. Quantum gates can operate on single or multiple qubits preserving the length. In other words, they perform unitary operations so that the norm of the new output state is 1. Thus, a generic quantum gate provides a way of doing unitary transformations on a state $|\psi\rangle$ and of producing an output state $|\psi'\rangle$:

$$|\psi'\rangle = U |\psi\rangle \quad (7)$$

where U denotes a unitary gate satisfying the following condition: $UU^\dagger = I$. The matrix multiplication of U with its conjugate transpose U^\dagger is equal to the identity matrix I . From the last statement, it can be deduced that it is possible to represent the quantum gates with matrices. So, (7) can be reformulated as matrix operations:

$$\begin{bmatrix} \alpha' \\ \beta' \end{bmatrix} = \begin{bmatrix} u_{00} & u_{01} \\ u_{10} & u_{11} \end{bmatrix} \begin{bmatrix} \alpha \\ \beta \end{bmatrix}, \quad u_{ij} \in \mathbb{C} \quad (8)$$

One of the most frequently used single-qubit quantum gate is X gate, which simply flips the state of the qubit. There also exist parametrized single-qubit gates such as RX, RY and RZ gates, which are the building blocks of variational quantum circuits. Each of those gates can manipulate the qubit state through a rotation of a specified angle θ around the corresponding axis. On the other hand, CNOT is a two-qubit gate, where one of the qubits is the control qubit and the other one is the target qubit. As long as the control qubit is in state $|1\rangle$, the target qubit is flipped. The graphical representations and the corresponding matrices for X, RY and CNOT gates are given in Table I.

TABLE I. FREQUENTLY USED QUANTUM GATES AND THEIR REPRESENTATIONS

Quantum Gate as a Matrix	Graphical Representation
$X = \begin{bmatrix} 0 & 1 \\ 1 & 0 \end{bmatrix}$	
$R_y(\theta) = \begin{bmatrix} \cos(\frac{\theta}{2}) & -\sin(\frac{\theta}{2}) \\ \sin(\frac{\theta}{2}) & \cos(\frac{\theta}{2}) \end{bmatrix}$	
$CNOT = \begin{bmatrix} 1 & 0 & 0 & 0 \\ 0 & 1 & 0 & 0 \\ 0 & 0 & 0 & 1 \\ 0 & 0 & 1 & 0 \end{bmatrix}$	

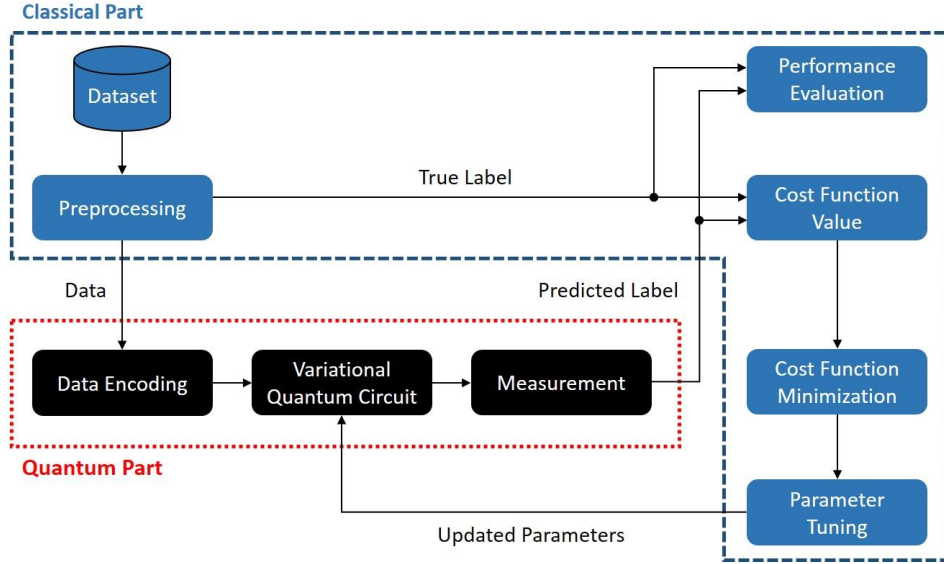


Fig. 2. Schematic representation of a variational quantum algorithm

C. Variational Circuits

As a machine learning model, variational quantum algorithms are comprised of quantum and classical computational resources, where the former includes the variational quantum circuits. This scheme introduces a hybrid quantum-classical approach in order to perform supervised learning tasks such as classification and regression. The main steps of a variational quantum algorithm depicted in Fig. 2 are as follows:

- Data preprocessing
- Mapping of data into a quantum state
- Transformation of the quantum state with a variational quantum circuit
- Generation of a predicted value through measurement
- Comparison of the predicted label and the true label using a cost function.
- Parameter tuning through optimization of the cost function
- Performance evaluation

IV. METHODOLOGY

In this section, the proposed variational quantum circuit is explained that is a part of the variational quantum algorithm. First of all, the employed dataset and its ingredients are introduced. The issues of scaling and normalization are the next steps before the features of a sample in the dataset are mapped into a quantum state. After the unitary transformation of the prepared quantum state is detailed, the cost function optimization will be described.

A. Dataset

This work utilizes a publicly available dataset [25, 26] obtained by observing the signal strengths of Wi-Fi routers positioned at different locations of a facility. Each sample in the dataset constitutes of seven signal values from the routers and a label corresponding to a location in the facility. In total, there are four labeled locations, each of which are numbered through 1 to 4 and there exist 500 samples for each of the classes. Some samples from the dataset are given in Table 2.

TABLE II. SAMPLE INSTANCES FROM THE DATASET

Router 1	Router 2	Router 3	Router 4	Router 5	Router 6	Router 7	Class
-63	-52	-56	-59	-66	-80	-80	1
-38	-55	-57	-41	-66	-73	-69	2
-51	-53	-54	-53	-62	-83	-82	3
-61	-52	-48	-61	-45	-90	-88	4

The location of a user possessing a mobile device is determined via monitoring the above mentioned router signals. Although the original dataset contains four different classes, we will be dealing with a binary classification task. So, we have only extracted class 1 and class 2 samples from the dataset.

B. Data Preprocessing

The mentioned dataset \mathcal{D} having m samples is a set of tuples $(x^{(i)}, y^{(i)})$, where $x^{(i)}$ denotes the feature vector and $y^{(i)}$ is the corresponding label for the i^{th} sample. There exist seven features in each sample and every feature in the feature vector $x^{(i)} = [x_1^{(i)}, x_2^{(i)}, \dots, x_7^{(i)}]^T$ is transformed by scaling it into the range $[0,1]$ with the following min-max scaler:

$$x_j^{(i)} = \frac{x_j^{(i)} - \min_j X}{\max_j X - \min_j X}, 1 \leq j \leq 7 \quad (9)$$

where $X = \{x^{(i)}\}_{i=1}^M$, $\min_j X$ and $\max_j X$ are the minimum and maximum of the j^{th} attribute in X , respectively; M is the number of samples in the dataset \mathcal{D} .

Since the quantum states have norm 1, before mapping the features into a quantum state, the scaled feature vector $x^{(i)}$ has to be normalized to unit length by updating each feature $x_j^{(i)}$ of $x^{(i)}$ (for the simplicity of the notation, the upperscript (i) in $x_j^{(i)}$ is omitted in the following equation):

$$x_j = \frac{x_j}{\sqrt{\sum_{k=1}^7 x_k^2}} \quad (10)$$

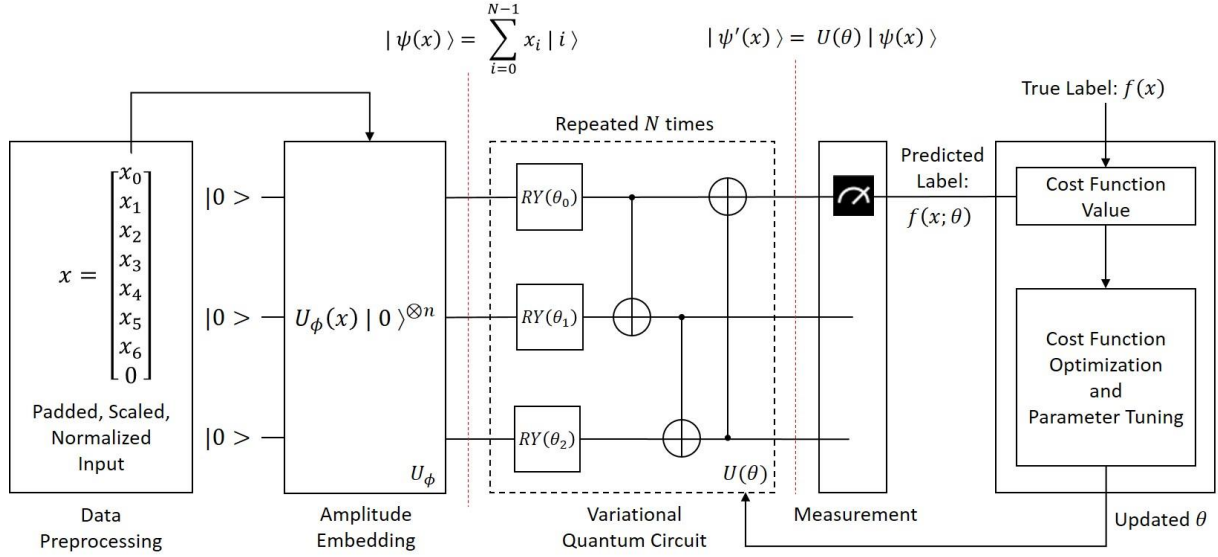


Fig. 3. Variational quantum algorithm applied on the user localization dataset

C. Data Encoding

A feature map used in classical machine learning approaches is a function ϕ that maps the data vectors in an input domain \mathcal{X} to a feature space domain \mathcal{X}' . The transformation of $\phi: \mathcal{X} \rightarrow \mathcal{X}'$ provides a better way of representing and manipulating data while dealing with supervised learning tasks. A similar approach is also available for quantum machine learning and is called as *quantum feature map*. The main logic behind a quantum feature map $\phi: x \in \mathcal{X} \rightarrow |\psi(x)\rangle \in \mathcal{H}$ is to transform the classical data into a quantum state, where the quantum state is described as a complex vector in the Hilbert space \mathcal{H} (see Section III.A). This mapping is in fact a unitary operation $U_\phi(x)$ applied on the initial state $|0\rangle^{\otimes n}$ using the vector x , where $|0\rangle^{\otimes n}$ denotes the tensor product of n -qubit $|0\rangle$ states.

Amplitude encoding [27] is one of the data encoding schemes in order to associate the classical data with the probability amplitudes of a quantum state. Supposing that the scaled and normalized feature vector $x = [x_0, \dots, x_{N-1}]$ is real and of dimension N satisfying the condition $2^n = N$, the amplitude encoding can be formally described as:

$$U_\phi(x): x \in \mathbb{R}^N \rightarrow |\psi(x)\rangle = \sum_{i=0}^{N-1} x_i |i\rangle \quad (11)$$

Here, $|i\rangle$ is the i^{th} computational basis state encoded in binary format. It has to be noted that the size of the feature vector in the user localization dataset is 7 and therefore all of the vectors have to be padded with a 0 so that the vector size is equated to an amplitude of 2. A further and important implication from the last statement is that the number of qubits required for amplitude encoding is $\lceil \log_2 N \rceil$.

D. Proposed VQC and Measurement Process

The main component of a VQA is the variational quantum circuit transforming the encoded input state $|\psi(x)\rangle$ into a new state $|\psi'(x)\rangle$. The parameter θ in the proposed VQC (Fig. 3), which is a vector of trainable parameters, is evolved during the learning phase. The unitary transformation $U(\theta)$

applied on $|\psi(x)\rangle$ is composed of the following gates: 1-qubit parametrized RY rotation and 2-qubit CNOT gates that provide the entanglement between the qubits in the circuit. The used VQC in this work is cascaded as multiple layers in order to allow the learning model to fit more complex functions and it is repeated N times in the QML model. The functionality of a VQC is formally described as:

$$|\psi'(x)\rangle = U(\theta) |\psi(x)\rangle \quad (12)$$

where $\theta = [\theta_1, \theta_2, \dots, \theta_m]$ and m is the number of parameters in the VQC.

The qubits in the circuit are numbered in a sequential manner from top to down. The top qubit is referred to as the least significant qubit. It is measured in the computational basis that is also known as a Pauli-Z measurement. Depending on the fact that the eigenvalues of the Pauli-Z gate are -1 and 1, the obtained measurements results are associated to continuous values in the range from -1 to 1.

The operator used in the measurement process is the observable \hat{B} of the quantum circuit. The expectation value $f(x; \theta)$ out of the measurement is the counterpart of the predicted label in the classical machine learning:

$$f(x; \theta) = \langle \psi'(x) | \hat{B} | \psi'(x) \rangle \quad (13)$$

Since the labels of the dataset are discrete values for the classification task (e.g., 1 for class 1 and 2 for class 2), the value of $f(x; \theta)$ has to be adjusted accordingly:

$$f(x; \theta) = \begin{cases} 1 & \text{if } f(x; \theta) < 0 \\ 2 & \text{if } f(x; \theta) \geq 0 \end{cases} \quad (14)$$

E. Postprocessing

The task of postprocessing is executed on the classical part of the variational quantum algorithm. Firstly, the predicted label and true label are passed to a cost function in order to quantify the error between the predicted and actual outcomes. This work utilizes the Mean Squared Error (MSE) as the cost function:

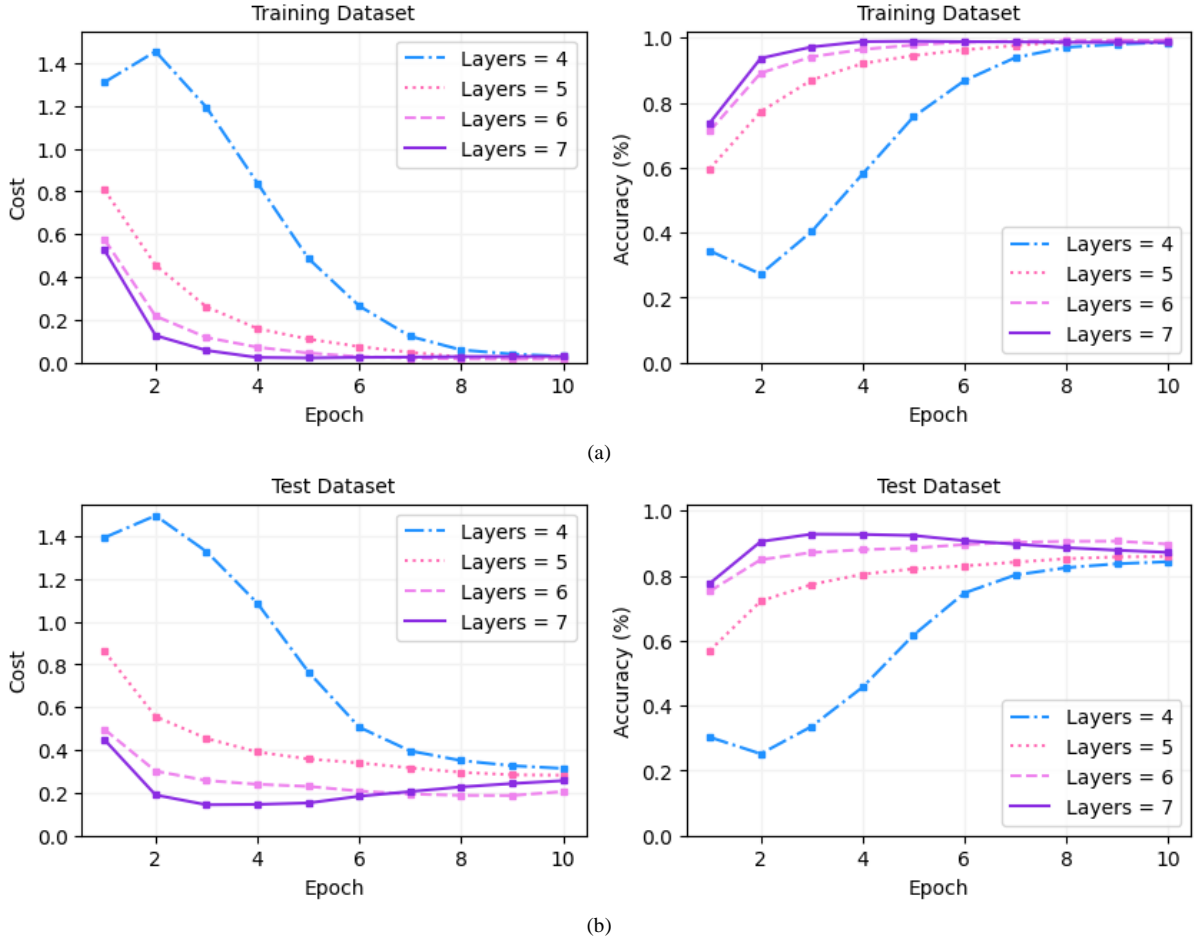


Fig. 4. Performance of the VQAs with different number of layers used in the corresponding VQCs. (a) Cost and accuracy values obtained for the training dataset. (b) Cost and accuracy values obtained for the test dataset.

$$J(\theta) = \frac{1}{2M} \sum_{i=1}^M (f(x^{(i)}; \theta) - f(x^{(i)}))^2 \quad (15)$$

where $x^{(i)}$ is the i^{th} sample in the dataset \mathcal{D} with M samples.

The calculation of the aggregate cost value is followed by an optimization on the cost function $J(\theta)$. The *Gradient Descent* approach is the employed optimization method, where the minimum of the function $J(\theta)$ is found by taking the partial derivative of this function with respect to the parameter vector θ and updating each parameter in θ simultaneously based on a learning rate η and the corresponding gradient:

$$\theta_j = \theta_j - \eta \frac{\partial}{\partial \theta_j} J(\theta) \quad (16)$$

The Gradient Descent routine is repetitively run until the parameter vector θ converges. On the other hand, the performance of the VQA is monitored through an accuracy metric, which is simply a measure for all of the labels predicted correctly:

$$\text{Accuracy} = \frac{\text{Number of correct predictions}}{\text{Total number of predictions}} \quad (17)$$

V. EXPERIMENTAL RESULTS

The user localization dataset includes 2000 samples and 4 classes in total. Those classes are associated to 4 different locations in a facility and there are 500 samples for each of the

class. Every sample is composed of 7 features related to the signal strengths received from 7 routers and a class label representing the location of the user. In consideration of a binary classification task, 800 samples are extracted from the dataset equally split between Class 1 and Class 2. On the other hand, 75% of the data is used for the training purpose, whereas the proposed learning model is validated with the rest of the data.

The simulations are carried out with PennyLane [28], a Python software framework for differentiable programming of quantum computers. It provides the necessary tools for the construction of gate-based quantum circuits, and in particular of the variational quantum circuit implemented in this work. In addition to the quantum computation based routines, PennyLane makes use of the classical optimization methods executed as a classical part of the hybrid quantum-classical environment.

To evaluate the performance, the proposed QML model is prepared as the VQA depicted in Fig. 3. First, each sample in the dataset is padded with 0 in order to meet the condition of having 8 amplitudes required for a 3-qubit quantum system. The padded samples are scaled and normalized, which is also mandatory due to the fact that all quantum states have a unit length of 1.

After the sample is mapped to a quantum state with the aid of amplitude encoding scheme, a unitary transformation of the quantum state is performed in the variational quantum circuit.

The experimental setup provides 4 variants of the VQA depending on the number of layers varying between the range 4 and 7. Each layer of the quantum circuit includes 3 RY rotation gates and 3 CNOT gates. Expectation values, which are the predictions, and the true labels are passed to the cost function aiming to determine the amount of error for the classification task. Next, a Gradient Descent Optimization takes place to obtain the best parameter values minimizing the cost function value. The updated parameters adjust the amount of qubit rotations in the VQC for the next iteration of the learning process.

The mentioned variational quantum algorithm variants with different number of VQC layers are compared in terms of cost and accuracy at every epoch. In total, there are 10 epochs, each of which includes 12 iterations since the training dataset of 600 samples are processed in batches of 50 samples. The means of cost and accuracy for each epoch are calculated through 12 iterations of the corresponding epoch.

The cost value for the VQA with 4-layered VQC is significantly higher than that of the other VQA variants in the early stages of the epochs for both of training and test datasets (Fig. 4). As the VQC parameters converge, it is obvious that all of the cost values decrease smoothly. It is almost zero in the case of training dataset, whereas cost of testing phase remains in the range between 0.2 – 0.4. Similarly, the outcome for the accuracy metric shows that all of the VQAs achieve a score of almost 100% during the training phase. However, the case differs for predicting the unseen labels such that the accuracy values rise without any fluctuation except for the 4-layered VQC until the range of 84% – 93% is reached. The highest achieved results are summarized in Table 3.

The best accuracy value throughout the test epochs is obtained at Epoch 3 when the 7-layered VQC is utilized. Nevertheless, its accuracy curve drops below the curve of the VQC with 6 layers, which is an indication of overfitting. This fact forces us to follow one of the two precautions to mitigate the overfitting issue: 1) The 7-layered VQC setup has to be stopped at earlier epochs through capturing a possible lower value of the next epoch. 2) Use directly the 6-layered VQC, which has 18 trainable parameters. Note that the VQCs with 4, 5, 6 and 7 layers contain 12, 15, 18 and 21 parameters, respectively.

TABLE III. BEST RESULTS FOR COST AND ACCURACY

VQC Layer Size	Training Dataset			Test Dataset		
	Cost	Accuracy	Epoch	Cost	Accuracy	Epoch
4	0.02889	0.98556	10	0.31417	0.84292	10
5	0.02000	0.99000	10	0.28250	0.85875	10
6	0.01611	0.99194	10	0.18750	0.90625	9
7	0.02167	0.98917	5	0.14417	0.92792	3

With the aim of emphasizing the true potential of variational quantum algorithms, the devised VQA is compared against the well-known machine learning algorithms such as Naïve Bayes, K-Nearest Neighbor, Logistic Regression and Support Vector Machine. It is observed that the VQCs with 6 and 7 layers perform better than the classical counterparts in terms of testing accuracy (Table 4). In relation to the training performances of compared algorithms, the 6-layered VQC achieves the second best result after the K-Nearest Neighbor algorithm.

TABLE IV. COMPARISON WITH WELL-KNOWN MACHINE LEARNING ALGORITHMS

Algorithms	Training Accuracy	Testing Accuracy
Naïve Bayes	0.99166	0.89500
K-Nearest Neighbor	0.99666	0.90500
Logistic Regression	0.99000	0.86500
Support Vector Machine	0.98666	0.84000
VQC with 6 Layers	0.99194	0.90625
VQC with 7 Layers	0.98917	0.92792

A software simulation environment with a lot of tunable parameters holds the disadvantage of longer execution times. At the same time, increasing the layer size or the depth of a quantum circuit and running it on a real quantum hardware of NISQ era may result in decoherence, which negatively affects the expected outcomes and degrades the performance. The major consequence of the simulation results is that the potential of quantum computing is evident for machine learning tasks. Also, the key component for solving large learning problems is likely to be the QML approaches with the advances in the fault tolerant quantum computers having more qubits than the NISQ devices.

VI. CONCLUSION

This work presented the design of a variational quantum algorithm consisting of data preprocessing, sample encoding, unitary evolution of quantum states, predictions based on measurement results, cost function optimization and parameter tuning. We especially focused on layered structure of the variational circuit employed in the proposed VQA. One of the foremost findings of this research is that the number of layers is of great importance to attain better results out of the classification task. Secondly, keeping the layer size at a reasonable amount is a key factor to mitigate the overfitting issue.

The implemented algorithm is evaluated with a publicly accessible dataset tackling with the problem of user localization. For detecting the actual locations of users possessing mobile devices, the signal strengths received from several routers are exploited. From the original dataset, we have extracted the samples associated with only two locations to present a two-label classifier scheme. The simulation results demonstrated the efficiency and applicability of quantum machine learning approaches on real world problems. An accuracy rate of 99% was achieved for the prediction of class 1 and class 2 labels during the learning stage. We furtherly observed that the performance of our VQA while evaluating with test samples was around 93% in terms of accuracy.

As a future direction, our research has to be extended to cover the multi-class classification ability on the employed dataset. This particularly requires a design update in the variational quantum circuit part. A further investigation can be maintained on the complex learning tasks with a bigger feature and sample space taking the limitations of near-term NISQ devices into the consideration. Furthermore, we plan to implement the developed quantum machine learning model on the cloud platforms, on which real quantum computers are accessible for public use.

CONTRIBUTION OF THE AUTHORS

The contributions of the authors to the article are equal.

CONFLICT OF INTEREST

There is no conflict of interest between the authors.

STATEMENT OF RESEARCH AND PUBLICATION ETHICS

Research and publication ethics were observed in this study.

REFERENCES

- [1] Michael A. Nielsen and Isaac Chuang, Quantum computation and quantum information. Cambridge, UK: Cambridge University Press, 2002.
- [2] Peter W. Shor, "Algorithms for quantum computation: discrete logarithms and factoring," in *Proc. 35th annual symposium on foundations of computer science*, 1994, pp. 124-134.
- [3] Lov K. Grover, "A fast quantum mechanical algorithm for database search," in *Proc. the twenty-eighth annual ACM symposium on Theory of computing*, 1996, pp. 212-219.
- [4] Seth Lloyd, "Universal quantum simulators," *Science*, vol. 273, no. 5278, pp. 1073-1078, Aug. 23, 1996.
- [5] Robin Harper, Steven T. Flammia, and Joel J. Wallman, "Efficient learning of quantum noise," *Nature Physics*, vol. 16, no. 12, pp. 1184-1188, Dec. 2020.
- [6] John Preskill, "Quantum computing in the NISQ era and beyond," *Quantum*, vol. 2, no. 79, pp. 1-20, Jul. 30, 2018.
- [7] Sukhpal Singh Gill *et al.*, "Quantum computing: A taxonomy, systematic review and future directions," *Software: Practice and Experience*, vol. 52, no. 1, pp. 66-114, Oct. 7, 2022.
- [8] N. Schetakakis, D. Aghamalyan, P. Griffin, and M. Boguslavsky, "Review of some existing QML frameworks and novel hybrid classical-quantum neural networks realising binary classification for the noisy datasets," *Scientific Reports*, vol. 12, no. 1, pp. 1-12, Jul. 13, 2022.
- [9] Maria Schuld and Francesco Petruccione, *Machine learning with quantum computers*, Berlin, Germany: Springer, 2021.
- [10] Tariq M. Khan and Antonio Robles-Kelly, "Machine learning: quantum vs classical," *IEEE Access*, vol. 8, pp. 219275-219294, Dec. 1, 2020.
- [11] L. Alchieri, D. Badalotti, P. Bonardi, and S. Bianco, "An introduction to quantum machine learning: from quantum logic to quantum deep learning," *Quantum Machine Intelligence*, vol. 3, pp. 1-30, Nov. 15, 2021.
- [12] S. Y. C. Chen and S. Yoo, "Federated quantum machine learning," *Entropy*, vol. 23, no. 4, pp. 1-15, Apr. 13, 2021.
- [13] Y. Du, T. Huang, S. You, M. H. Hsieh, and D. Tao, "Quantum circuit architecture search: error mitigation and trainability enhancement for variational quantum solvers," 2020, *arXiv:2010.10217*.
- [14] T. Hubregtsen, J. Pichlmeier, P. Stecher, and K. Bertels, "Evaluation of parameterized quantum circuits: on the relation between classification accuracy, expressibility, and entangling capability," *Quantum Machine Intelligence*, vol. 3, pp. 1-19, Mar. 11, 2021.
- [15] Samuel Yen-Chi Chen *et al.*, "Variational quantum circuits for deep reinforcement learning," *IEEE Access*, vol. 8, pp. 141007-141024, Jul. 20, 2020.
- [16] A. Al-Habashna, G. Wainer, and Moayad Aloqaily, "Machine learning-based indoor localization and occupancy estimation using 5G ultra-dense networks," *Simulation Modelling Practice and Theory*, vol. 118, pp. 1-17, 2022.
- [17] P. S. Varma and Veena Anand, "Fault-Tolerant indoor localization based on speed conscious recurrent neural network using Kullback-Leibler divergence," *Peer-to-Peer Networking and Applications*, vol. 15, no. 3, pp. 1370-1384, Feb. 25, 2022.
- [18] K. Ngamakeur, S. Yongchareon, J. Yu, and S. Islam, "Passive infrared sensor dataset and deep learning models for device-free indoor localization and tracking," *Pervasive and Mobile Computing*, vol. 88, pp. 1-16, 2023.
- [19] J. Xue, J. Liu, M. Sheng, Y. Shi, and J. Li, "A WiFi fingerprint based high-adaptability indoor localization via machine learning," *China Communications*, vol. 17, no. 7, pp. 247-259, Jul. 24, 2020.
- [20] M. Schuld, I. Sinayskiy, and F. Petruccione, "Quantum computing for pattern classification," in *Proc. Trends in Artificial Intelligence: 13th Pacific Rim Int. Conf. Artificial Intelligence*, Gold Coast, QLD, Australia, Dec. 1-5, 2014, pp. 208-220.
- [21] Y. Wang, Y. Wang, C. Chen, R. Jiang, and W. Huang, "Development of variational quantum deep neural networks for image recognition," *Neurocomputing*, vol. 501, pp. 566-582, Aug. 28, 2022.
- [22] S. Otgonbaatar and M. Datcu, "Classification of remote sensing images with parameterized quantum gates," *IEEE Geoscience and Remote Sensing Letters*, vol. 19, pp. 1-5, Sep. 9, 2021.
- [23] M. M. Hossain, M. A. Rahim, A. N. Bahar, and M. M. Rahman, "Automatic malaria disease detection from blood cell images using the variational quantum circuit," *Informatics in Medicine Unlocked*, vol. 26, pp. 1-14, Oct. 1, 2021.
- [24] M. Schuld, A. Bocharov, K. M. Svore, and N. Wiebe, "Circuit-centric quantum classifiers," *Physical Review A*, vol. 101, no. 3, Mar. 6, 2020.
- [25] R. Bhatt, Fuzzy-rough approaches for pattern classification: hybrid measures, mathematical analysis, feature selection algorithms, decision tree algorithms, neural learning, and applications, Amazon Books, 2005.
- [26] J. G. Rohra, B. Perumal, S. J. Narayanan, P. Thakur, and R. B. Bhatt, "User localization in an indoor environment using fuzzy hybrid of particle swarm optimization & gravitational search algorithm with neural networks," in *Proc. Sixth Int. Conf. Soft Computing for Problem Solving*, in *Advances in Intelligent Systems and Computing*, vol. 546, pp. 286-295, Feb. 24, 2017.
- [27] Maria Schuld, "Supervised quantum machine learning models are kernel methods," 2021, *arXiv:2101.11020*.
- [28] Ville Bergholm *et al.*, "Pennylane: Automatic differentiation of hybrid quantum-classical computations," 2018, *arXiv:1811.04968*.